IEEE Trans. Power Systems, Vol. 14, No. 1, February 1999, pp. 158-165.

Analysis of SVC and TCSC Controllers in Voltage Collapse

Claudio A. Cañizares
Member, IEEE
University of Waterloo
Department of Electrical & Computer Engineering
Waterloo, ON, Canada N2L 3G1
claudio@iliniza.uwaterloo.ca

Zeno T. Faur
SAF Drive Systems Ltd.
88 Ardelt Ave.
Kitchener, ON, Canada N2C 2C9
zfaur@sstech.on.ca

Abstract—This paper presents detailed steady-state models with controls of two Flexible AC Transmission System (FACTS) controllers, namely, Static Var Compensators (SVCs) and Thyristor Controlled Series Capacitors (TCSCs), to study their effect on voltage collapse phenomena in power systems. Based on results at the point of collapse, design strategies are proposed for these two controllers, so that their location, dimensions and controls can be optimally defined to increase system loadability. A European system is used to illustrate the application of all proposed models and techniques.
Keywords: FACTS, SVC, TCSC, voltage collapse, loadability margin, bifurcations.

I. Introduction

Voltage collapse problems in power systems have been a permanent concern for the industry, as several major blackouts throughout the world have been directly associated to this phenomenon, e.g., Belgium 1982, WSCC July 1996, etc. Many analysis methodologies have been proposed and are currently used for the study of this problem, as recently reported in [1, 2, 3]. Most of these techniques are based on the identification of system equilibria where the corresponding Jacobians become singular; these equilibrium points are typically referred to as points of voltage collapse and can be mathematically associated to saddle-node bifurcation points [4, 5].

The collapse points are also known as maximum loadability points; in fact, the voltage collapse problem can be restated as an optimization problem where the objective is to maximize certain system parameters typically associated to load levels [6, 7, 8, 9]. Hence, voltage collapse techniques may also be used to compute the maximum power that can be transmitted through the transmission system, also known in the new competitive energy market as Total Transfer Capability or as Available Transfer Capability (ATC) [10].

It is well known that shunt and series compensation can be used to increase the maximum transfer capabilities of power networks [11]. With the improvements in current and voltage handling capabilities of power electronic devices that have allowed for the development of Flexible AC Transmission Systems (FACTS), the possibility has arisen of using different types of controllers for efficient shunt and series compensation. Thus, FACTS controllers based on thyristor controlled reactors (TCRs), such as Static Var Compensators (SVCs) and Thyristor Controlled Series Capacitors (TCSCs), are being used by several utilities to compensate their systems [12]. More recently, various types of controllers for shunt and series compensation, based on voltage source inverters (VSIs), i.e., Shunt and Series Static Synchronous Compensators (STATCOMs and SSSCs) and Unified Power Flow Controllers (UPFCs), have been proposed and developed [13]. This paper concentrates on thoroughly studying the effecst of SVCs and TCSCs on voltage collapse studies by using adequate steady-state models of these controllers.

In [14], the authors use standard voltage collapse analysis tools to study the effect in the maximum load margin of the location of a given SVC; an approximate SVC model is used for the computations. In [15], the authors use approximate SVC and TCSC models together with typical collapse computational tools and optimization techniques to determine the appropriate location and size of these controllers; dynamic simulations using more detailed models are then performed to study the effect of these controllers in the overall stability of the network. The authors of the current paper present in [16] a first attempt to adequately model SVCs and TCSCs for the study of voltage collapse phenomena; techniques are proposed to determine adequate design parameters, particularly location, to produce a "maximum" increment in the loadability margin. In the current paper, better models and new methodologies are proposed, especially for the TCSC, with the aim of producing optimal improvements in the loadability margin. Furthermore, the effect of SVC and TCSC sizing, i.e., compensation levels, in the loading margin, which is discussed in general for shunt and series compensation in [17], is specifically addressed in this paper.

Section II briefly introduces the basic mathematical tools required for the analysis of voltage collapse phenomena, and presents a detailed description of the SVC and TCSC models proposed for these types of studies. In Section III the techniques proposed for determining optimal SVC and TCSC design parameters such as size and location are discussed; the real test system used for the illustration of all proposed techniques and models is also described in this section. Finally, Section IV summarizes the main points of this paper and discusses future research directions.

II. Modeling

Voltage collapse studies and their related tools are typically based on the following general mathematical description of the system:

$$\begin{aligned} \dot{x} &= f(x, y, \lambda, p) \\ 0 &= g(x, y, \lambda, p) \end{aligned} \tag{1}$$

where $x \in \Re^n$ represents the system state variables, corresponding to dynamical states of generators, loads, and any

other time varying element in the system, such as FACTS controllers; $y \in \Re^n$ corresponds to the algebraic variables, usually associated to the transmission system and steady-state element models, such as some generating sources and loads in the network; $\lambda \in \Re^l$ stands for a set of uncontrolled parameters that drive the system to collapse, which are typically used to represent the somewhat random changes in system demand. Vector $p \in \Re^k$ is used here to represent system parameters that are directly controllable, such as shunt and series compensation levels.

Based on (1), the collapse point may be defined, under certain assumptions, as the equilibrium point where the related system Jacobian is singular, i.e., the point $(x_o, y_o, \lambda_o, p_o)$ where

$$\left[\begin{array}{c} f(x,y,\lambda,p) \\ g(x,y,\lambda,p) \end{array} \right] = F(z,\lambda,p) = 0$$

and $D_z F|_o$ has a zero eigenvalue [18]. This equilibrium is typically associated to a saddle-node bifurcation point.

For a given set of controllable parameters p_o, voltage collapse studies usually concentrate on determining the collapse or bifurcation point (x_o, y_o, λ_o), where λ_o typically corresponds to the maximum loading level or loadability margin in p.u., %, MW, MVar or MVA, depending on how the load variations are defined. Based on bifurcation theory, two basic tools have been developed and applied to the computation of this collapse point, namely, direct and continuation methods [19].

Since one is mostly interested in the collapse point and its related zero eigenvalues and eigenvectors, it has been shown in [20] that not all dynamical equations are of interest; precise results may be obtained if the set of equations used in the computation of the collapse point adequately represent the equilibrium equations of the full dynamical system. Control limits are of great importance in this case, as these have a significant effect on the values of $(x_o, y_o, \lambda_o, p_o)$; this has been clearly illustrated for generators in [21, 22]. In the case of FACTS controllers, this implies that adequate controller models must accurately reproduce steady-state behavior and control strategies, including all associated limits; the inadequate representation of SVC and TCSC controlers has been the main shortcoming of most of the previous papers that discuss the effect of these controllers in voltage collapse [14, 15]. Hence, the following models are proposed for the correct representation of SVCs and TCSCs in voltage collapse studies.

A. SVC

The two most popular configurations of this type of shunt controller are the fixed capacitor (FC) with a thyristor controlled reactor (TCR), and the thyristor switched capacitor (TSC) with TCR [23]. Of these two setups, the second (TSC-TCR) minimizes standby losses; however, from a steady-state perspective, this is equivalent to the FC-TCR. Therefore, the FC-TCR structure depicted in Fig. 1 is the one used in this paper to develop the desired models. The TCR consists of a fixed (usually air-core) reactor of inductance L and a bi-directional thyristor valve. The thyristor valves are fired symmetrically in an angle α control range of 90° to 180°, with respect to the capacitor (inductor) voltage. The valves automatically turn off at approximately the zero crossings of the ac current.

Assuming that the controller voltage, which for the SVC is the bus voltage, is sinusoidal, and performing a Fourier series analysis on the inductor current waveform, the TCR

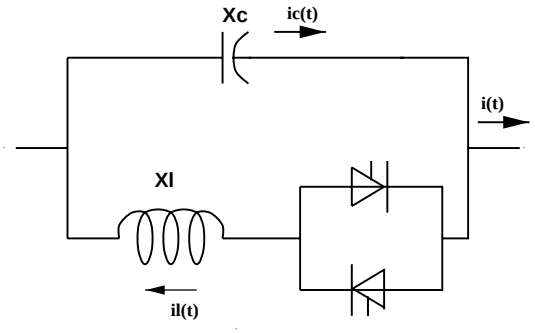

Fig. 1. Common structure for SVC and TCSC.

at fundamental frequency can be readily demonstrated to be equivalent to a variable inductance X_V given by [24, 25]

$$X_V = X_L \frac{\pi}{2(\pi - \alpha) + \sin 2\alpha}$$

where X_L is the fundamental frequency reactance of the inductor without thyristor control, and α is the firing angle of the valves with respect to the zero crossing of the controller voltage. Hence, the total equivalent impedance X_e of the controller may be represented by

$$X_e = X_C \frac{\pi / r_x}{\sin 2\alpha - 2\alpha + \pi(2 - 1/r_x)} \qquad (2)$$

where $r_x = X_C / X_L$. The limits of the controller are given by the firing angle limits, which are fixed by design.

In a three-phase system, three single phase thyristor controlled reactors are used in delta connection. A step down transformer is required in HV or EHV applications as the TCR voltage is limited for technical and economic reasons to 50 kV or below [26].

The typical steady-state control law of a SVC used here is depicted in Fig. 2, and may be represented by the following voltage-current characteristic:

$$V = V_{REF} + X_{SL}\, I$$

where V and I stand for the total controller RMS voltage and current magnitudes, respectively, and V_{REF} represents a reference voltage. Typical values for the slope X_{SL} are in the range of 2 to 5 %, with respect to the SVC base; this is needed to avoid hitting limits for small variations of the bus voltage. A typical value for the controlled voltage range is ±5% about V_{REF} [26, 27]. At the firing angle limits, the SVC is transformed into a fixed reactance.

B. TCSC

From a steady-state perspective, the structure of the controller is equivalent to the FC-TCR SVC illustrated in Fig. 1. However, the equivalent impedance of the TCSC at 60 Hz is more appropriately represented by assuming a sinusoidal steady-state total current rather than a sinusoidal voltage [28]. In that case, the equivalent impedance may be modeled using the following equation [28]:

$$\begin{aligned} X_e \;=\; & -X_C \left[1 - \frac{k_x^2}{k_x^2 - 1} \frac{\sigma + \sin\sigma}{\pi} \right. \\ & \left. + \frac{4k_x^2 \cos^2(\sigma/2)}{\pi(k_x^2 - 1)^2} \left(k_x \tan\frac{k_x \sigma}{2} - \tan\frac{\sigma}{2} \right) \right] \end{aligned} \qquad (3)$$

where $\sigma = 2(\pi - \alpha)$ and $k_x = \sqrt{r_x} = \sqrt{X_C/X_L}$.

Figure 3 depicts the values of X_e obtained from both (2) and (3) for different values of firing angle α, for a typical TCSC ratio of $r_x = 10$ [12]. Notice that there is a value of $\alpha = \alpha_r$ that causes steady-state resonance, i.e., $X_V = X_C$; $\alpha_r = 143.6°$ for (2), and $\alpha_r = 151.5°$ for (3). Different values of r_x yield different resonant points. The device can be continuously controlled in the capacitive or inductive zone, avoiding the steady-state resonance region; this type of control is called Vernier control.

For the SVC, resonance is not a problem, as it is shunt connected to the system and, hence, at the resonant point the controller is basically switched off the system without any notable effects. Furthermore, the bus voltage harmonic content is not significantly affected by changes in α. Thus, the steady-state limits of the firing angle for this controller are $90° < \alpha < 180°$.

For the TCSC, which is connected in series with a transmission line, the resonant point must be avoided to prevent harmonic problems and large internal currents that may damage the controller, as well as avoid line current interruption. Operation of this controller "close" to the resonant point is not practical in steady-state either, as this may induce substantial harmonics in the line current [25]. Finally, steady-state TCSC operation in the inductive region is atypical, as this would be equivalent to reducing the transmission system capability, while yielding voltages with high harmonic content [25]. Hence, the steady-state limits for the firing angle in this case may be defined as $\alpha_r < \alpha < 180°$.

Figure 3 also depicts the equivalent susceptance $B_e = -1/X_e$ versus α. Observe that B_e presents a significantly better numerical profile for changes in α than X_e; in other words, B_e varies more smoothly with respect to α. For this reason, all system equations are implemented using the susceptance equations rather than the corresponding reactance equations.

C. *Steady-state Equations and Limits*

1. *SVC*

The SVC is usually connected to the transmission system through a step-down transformer, which is treated in a similar manner as other transformers in the system. The SVC with its corresponding parameters is schematically presented in Fig. 4; the controlled voltage is typically V_l. Equations (4) below accurately describe the steady-state behavior of the SVC when connected to a system bus k.

$$\begin{aligned} V_l - V_{REF} + X_{SL} V_k B_e &= 0 \quad (4) \\ Q_{SVC} - V_k^2 B_e &= 0 \\ \pi X_C X_L B_e + \sin 2\alpha - 2\alpha + \pi \left(2 - \frac{X_L}{X_C}\right) &= 0 \end{aligned}$$

These equations are numerically well behaved. The initialization of the SVC variables is done either from a "flat start," or from a user defined initial guess. This flat start is based on the initial values of ac variables and the characteristic of the equivalent reactance (Fig. 3). Thus, the impedance is initialized at the resonant point $X_V = X_C$, i.e., $Q_{SVC} = 0$. The firing angle α is initialized at 92°, which has proved to be a good starting point (convergence wise) in several test systems at various loading conditions.

The SVC control limits are basically represented as limits on the firing angle α, i.e., $\alpha \epsilon [\alpha_m, \alpha_M]$, where α_m is the minimum firing angle and α_M is the maximum firing angle.

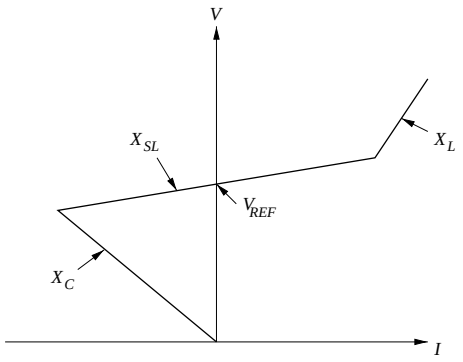

Fig. 2. SVC steady-state control scheme.

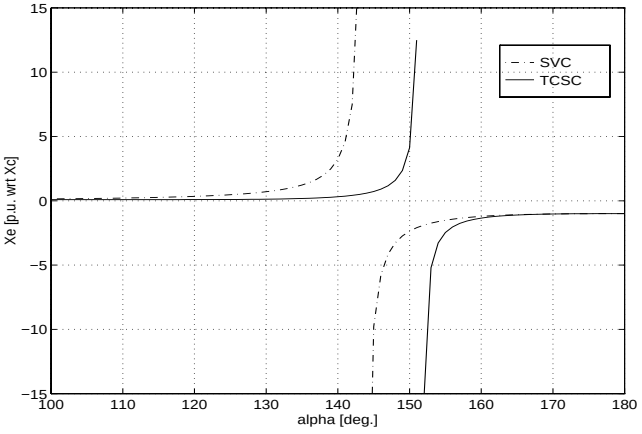

(a)

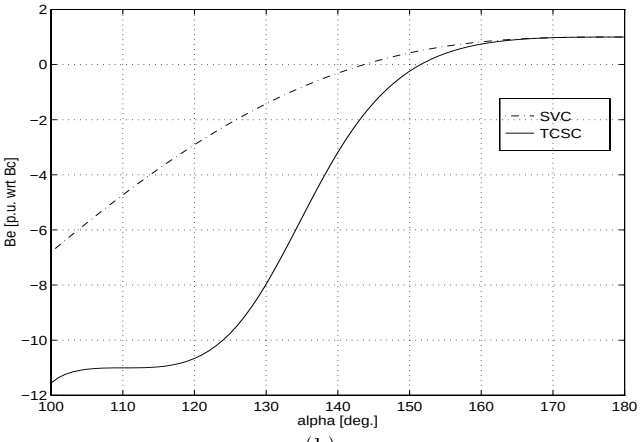

(b)

Fig. 3. Equivalent (a) reactance X_e and (b) susceptance Be of the FC-TCR controller.

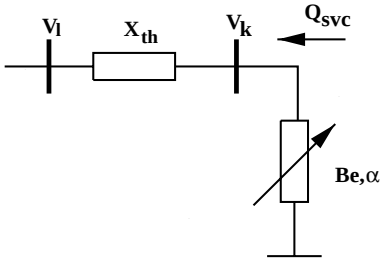

Fig. 4. SVC steady-state circuit representation.

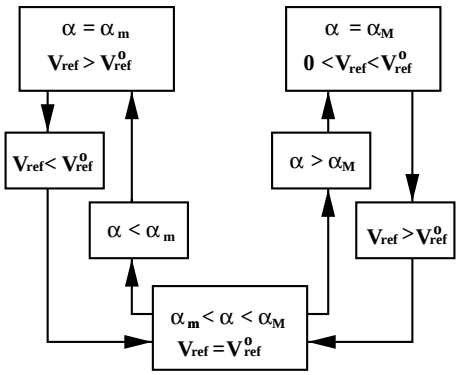

Fig. 5. Handling of SVC limits.

If there is no solution within these limits, the firing angle is fixed at the corresponding limit and V_{REF} is then allowed to change. This procedure, depicted in Fig. 5, allows for the use of the same set of equations when the SVC is at its limits, thus simplifying the solution process. Moreover, by solving for the variable V_{REF} when α hits a limit, the SVC may regain voltage control if the interaction with the rest of the system brings V_l within the controllable region. Although this paper only considers limits on the firing angle α, as is the case in the actual control system, other steady-state limits may be imposed on some of the other variables in (4), such as limits on the bus voltage or reactive power compensation levels.

2. TCSC

The TCSC is assumed to be connected between buses k and m, as illustrated in Fig. 6. The controller model is lossless, i.e., the active power P at node k is the same as the power at node m. Thus, the steady-state behavior of this controller may be modeled by the following set of equations:

$$\begin{aligned}
P + V_k V_m B_e \sin(\theta_k - \theta_m) &= 0 \quad (5)\\
-V_k^2 B_e + V_k V_m B_e \cos(\theta_k - \theta_m) - Q_k &= 0\\
-V_m^2 B_e + V_k V_m B_e \cos(\theta_k - \theta_m) - Q_m &= 0\\
B_e - \pi \left(k_x^4 - 2k_x^2 + 1\right) \cos k_x(\pi - \alpha)/ & \\
\left[X_C \left(\pi\, k_x^4 \cos k_x(\pi - \alpha)\right.\right. & \\
-\pi \cos k_x(\pi - \alpha) - 2\, k_x^4 \alpha \cos k_x(\pi - \alpha) & \\
+2\,\alpha\, k_x^2 \cos k_x(\pi - \alpha) - k_x^4 \sin 2\alpha \cos k_x(\pi - \alpha) & \\
\left.\left.+k_x^2 \sin 2\alpha \cos k_x(\pi - \alpha) - 4\, k_x^3 \cos^2\alpha \sin k_x(\pi - \alpha)\right.\right. & \\
\left.\left.-4\, k_x^2 \cos\alpha \sin\alpha \cos k_x(\pi - \alpha)\right)\right] &= 0\\
\sqrt{P^2 + Q_k^2} - I\, V_k &= 0\\
\theta_k - \theta_m - \delta_t &= 0
\end{aligned}$$

where the equation for B_e is the result of inverting (3). The control mode is defined by one of the following equations, depending on the type of control chosen:

- Reactance control: $B_{SET} - B_e = 0$
- Power control: $P_{SET} - P = 0$
- Current control: $I_{SET} - I = 0$
- Transmission angle control: $\delta_{SET} - \delta_t = 0$

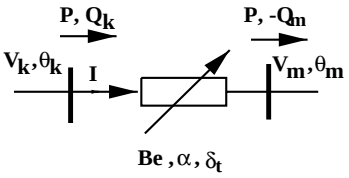

Fig. 6. TCSC steady-state circuit representation.

As in the case of the SVC, only limits on the firing angle α are considered here; however, other controller limits, such as maximum TCSC series voltage, may be directly applied to the different variables in (5).

The "flat start" initialization of the TCSC variables is based on its design constraints, the equivalent reactance characteristic, and the firing angle limits. Based on several system tests, the TCSC initial value process assumes an initial $\alpha = 160°$, and then proceeds to calculate the rest of the TCSC variables based on the initial values of the ac variables and equations (5). This initial value of the firing angle was determined so that it is typically not close to the resonant point, and has provided a robust starting point for a wide range of loading conditions in several test systems.

The TCSC control limits are basically limits on the firing angle α. If α hits a limit, the firing angle is fixed at the corresponding limit and the control mode is simply switched to reactance control.

III. Results

A real European system was used as a test system to try the models and techniques proposed in this paper; a one-line sketch of this system is depicted in Fig. 7. The system has 560 buses, 129 generator buses, 723 lines and transformers, and 14 areas; the power mainly flows from north to south. The generators are modeled as standard PV buses with both P and Q limits; loads are represented as constant PQ loads; the LTCs are kept fixed at their initial positions. The P and Q load powers are not voltage dependent and are assumed to change as follows:

$$P_L = P_{L_o}(1 + \lambda\, k_P) \quad (6)$$

$$Q_L = Q_{L_o}(1 + \lambda\, k_Q) \quad (7)$$

where P_{L_o} and Q_{L_o} represent the initial loading condition; $k_P = k_Q = 2.5$ for all loads in the two main load areas, which will be referred to as Area 1 and Area 2, while $k_P = k_Q = 1$ for the rest of the system, i.e., the loads in these two areas are considered to increase at a rate 2.5 higher than in the rest of the system. This load representation is used for "negative" loads as well, which are used to model ac links feeding the system from neighboring countries. Generators supply the active power required by the system load changes, within allowed limits, at the same level as their own initial loading conditions. There is no area power flow control in this system.

The data used here is characterized by a relatively low initial load demand (net load, considering "negative" loads, of about 19 GW), with several 380 kV lines switched off the network for either maintenance purposes or to avoid system overvoltages. Simulating an actual event, a blackout occurs when the main 380 kV link between Areas 1 and

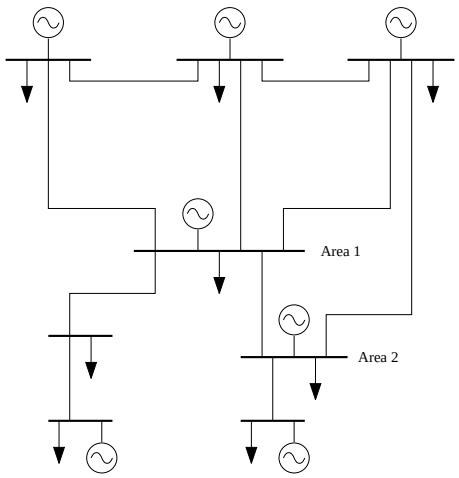

Fig. 7. One-line sketch of test system.

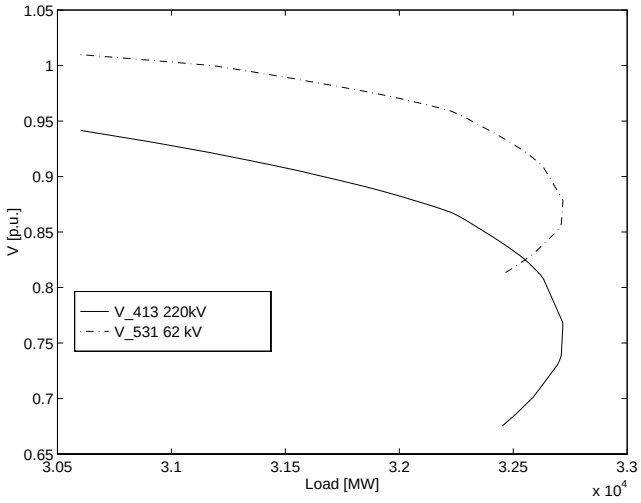

Fig. 8. Base case voltage profiles.

2, which in this case corresponds to the line with the highest loading level, is tripped off, as the post-contingency equilibrium point is lost in this case for the given load model. Thus, based on voltage collapse theory, the only way to recover solvability when this line is removed and, hence, recover the system, without adding new transmission paths, is to shed load. Adding SVCs and/or TCSCs to this system is probably not sufficient either to recover steady-state solvability in this case, as confirmed by the results shown below for the system with FACTS controllers.

Figure 8 depicts the voltage profiles of two buses identified as "critical," namely, bus 413 (220kV) in Area 1 and bus 531 (62kV) in Area 2. The system presents a collapse or maximum loading point, where the system Jacobian becomes singular, at $\lambda_o = 0.06928$ p.u., which is equivalent to a 2120 MW or 11 % increase in net load. Based on the largest entries in the right and left eigenvectors associated to the zero eigenvalue at the collapse point, bus 413 is identified as the "critical voltage bus" needing Q support, whereas bus 531 is identified as the "critical angle" bus needing P support.

A. SVC

Based on this collapse analysis, bus 413 is targeted as the first location for an SVC. The compensation level or MVar size of the SVC is chosen based on the reactive power needed to maintain the corresponding bus voltage at 0.95 p.u. (minimum estimated SVC voltage control range) for the loading condition defined by the collapse point value of $\lambda = \lambda_o = 0.06928$ p.u. This power is calculated by computing a new equilibrium point for the system where the desired bus is treated as a PQ bus; the power computed this way is 228 MVar. Assuming that the inductive rating of the SVC is equal to its capacitive range, the SVC rating is then chosen to be $Q_{SVC} = \pm 228$ MVar. A SVC control slope of 2 % is selected, and the step-down transformer is assumed to be 220/26 kV, with an equivalent reactance of 10 % with respect to the SVC base. These are all typical values of SVC parameters and associated step-down transformers [27].

The results of locating the SVC at the desired bus are depicted in the voltage profiles of Fig. 9. Observe the "flatter" voltage profile when the SVC is added to the system, rendering this voltage as an inadequate measure of proximity to collapse; there are more adequate indices that have been developed for this purpose [3]. The sharp change in bus voltage is due to SVC limits. The new maximum loading condition in this case is $\lambda_o = 0.08865$p.u. $= 2713$ MW. As shown in [14, 16], the maximum loading margin does not increase as much when the same SVC is moved to a bus that does not belong to the critical voltage area, e.g., for bus 531, $\lambda_o = 0.07274$p.u. $= 2226$ MW.

Figure 10 illustrates the effect of the MVar rating on the maximum system load for an SVC located at the critical bus. One might think that the larger the SVC, the greater the increase in the maximum load, as suggested in [15] and somewhat supported by the results presented in [17]; however, in [9], the author shows that there is a maximum increase in load margin with respect to the compensation level. This is clearly depicted in Fig. 10, where the maximum load reaches a "plateau" at about 340 MVar, due to generators' P and Q limits, which significant affect the dispatch scenario.

In order to better evaluate the "optimal" SVC rating level, the following performance level is proposed [25]:

$$f_p = \frac{\lambda_o \text{ [MW]}}{Q_{SVC} \text{ [MVar]}} \tag{8}$$

This ratio shows the effect of the SVC MVar rating on the maximum system load; therefore, a maximum value of f_p yields the optimal SVC rating, as this point corresponds to the maximum load increase at the minimum MVar compensation level. Thus, from Fig. 10(b), one can conclude that a ± 340 MVar SVC is the optimal for this system.

B. TCSC

A similar approach to the one followed to analyze the SVC effect in maximum loadability is used to study the corresponding effects of a TCSC. Thus, based on the maximum entries in the "zero" eigenvectors at the collapse point, the area around bus 531 is identified as requiring P support. However, when a TCSC is added to compensate the reactance of the main line feeding this area, there is no significant change on the value of λ_o, i.e., the loading level at which collapse occurs remains effectively the same ($\lambda_o = 0.06930$p.u. $= 2121$ MW for a 50 % compensation level). The main reason for this phenomenon is that

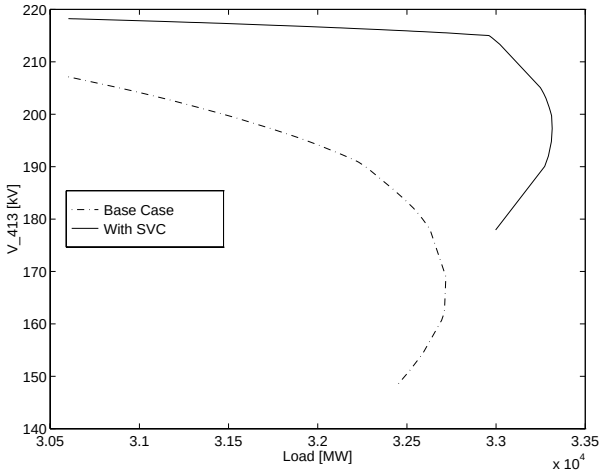

Fig. 9. Voltage profile for 228 MVar SVC at critical bus 413 (220kV).

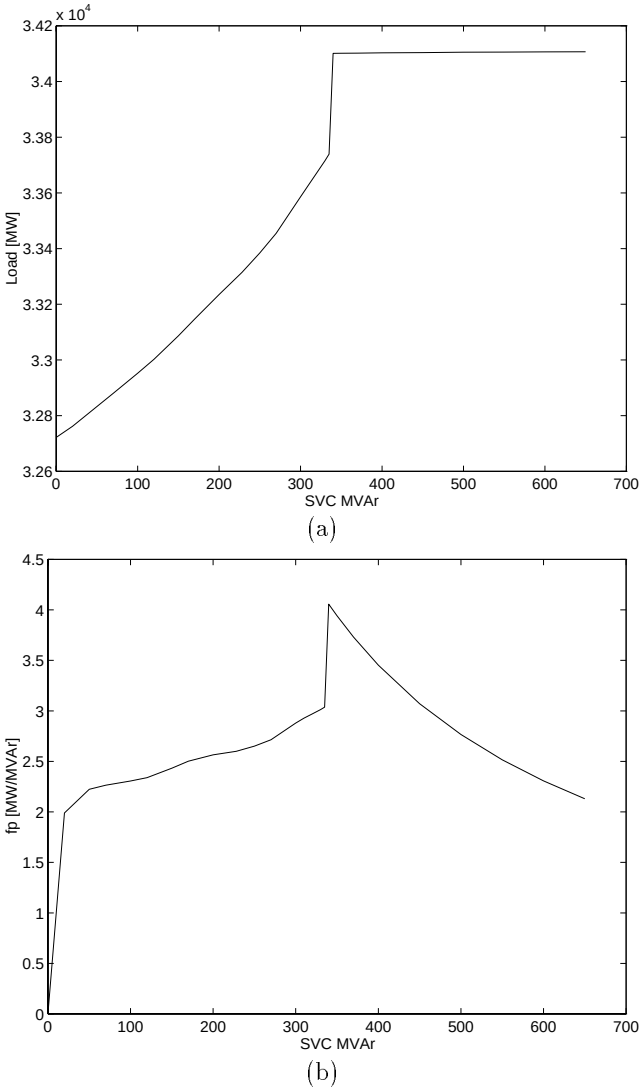

Fig. 10. Effect of changing SVC compensation levels at critical bus 413 in (a) loading margin and (b) performance measure fp.

the loading level of this line between the base load and the collapse point remains basically unchanged. When the TCSC is used to compensate by a typical 50 % the reactance of *the line that presents the largest increase in power at the point of collapse*, i.e., the main 380 kV line connecting buses 409 in Area 1 and 436 in Area 2 which triggered the system collapse in 1994, the maximum loading margin is significantly increased to $\lambda_o = 0.11549$p.u. $= 3534$ MW. The effect of this TCSC on the voltage profile of bus 413 is illustrated in Fig. 11. Observe the steady bus voltage decline as there is no direct voltage control of this bus; the flat voltage profile when close to collapse is due to a combination of P and Q limits that significantly affect the power flow pattern, changing the critical area of the system. (This particular voltage behavior requires more studies to better understand this phenomenon.)

Figures 12 depict of effect of TCSC compensation level on the loading margin and the performance factor f_p, which is defined based on (8) as

$$f_p = \frac{\lambda_o \text{ [MW]}}{X_{set} \text{ [\% of } X_{line}\text{]}} \tag{9}$$

These results are rather similar to the ones depicted for the SVC in Fig. 10, i.e., there is a somewhat linear dependency of the maximum loading margin with respect to the compensation level, with f_p showing a maximum value at about 34 %.

Other TCSC control techniques such as angle, power, or current control are not really appropriate for these types of applications, as these control strategies fix the corresponding variables at a given value, not allowing them to vary as the load changes and, hence, limiting the power that can be transmitted through the controlled line. This typically results in a reduced value of λ_o [16].

IV. Conclusions

Adequate models and related equations for representing SVCs and TCSCs in steady-state studies, particularly voltage collapse, are presented and thoroughly discussed in this paper. Based on voltage collapse theory, techniques for optimally locating and dimensioning these controllers are proposed and illustrated in a real system. The results presented in this paper clearly show how SVCs and TCSCs can be used to increase system loadability in practical applications.

Feasibility studies carried out by utilities typically show that similar improvements in transfer capabilities may be obtained using mechanically operated shunt and series compensation, at significant lower initial costs. However, is well known that these FACTS controllers have the additional advantage of being able to control "fast" system oscillations due to their quick response; furthermore, maintenance costs are lower, as there are no mechanical switches to worry about in these controllers. Hence, by properly modeling these controllers in transient stability programs, it would be interesting to determine any other possible advantages of these controllers in voltage stability studies.

The authors are currently working on developing appropriate models for other FACTS controllers, namely, STATCOM, SSSC and UPFC, for transient and steady-state stability analyses, to also analyze the advantages and disadvantages of these controllers in voltage stability studies.

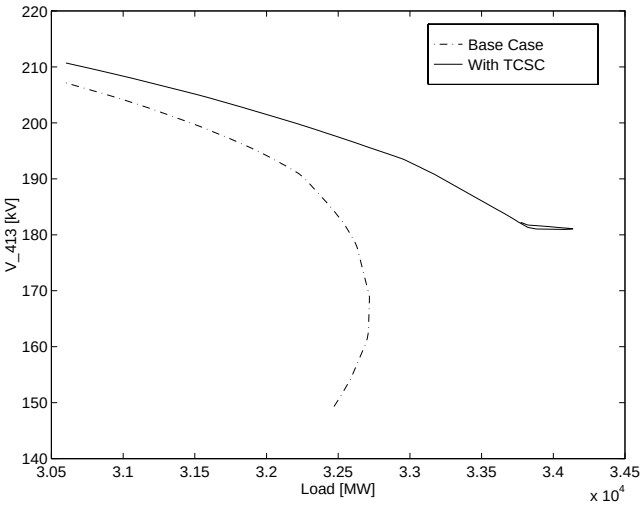

Fig. 11. Voltage profile for TCSC at 50% reactance compensation level critical line 409-436 (380 kV).

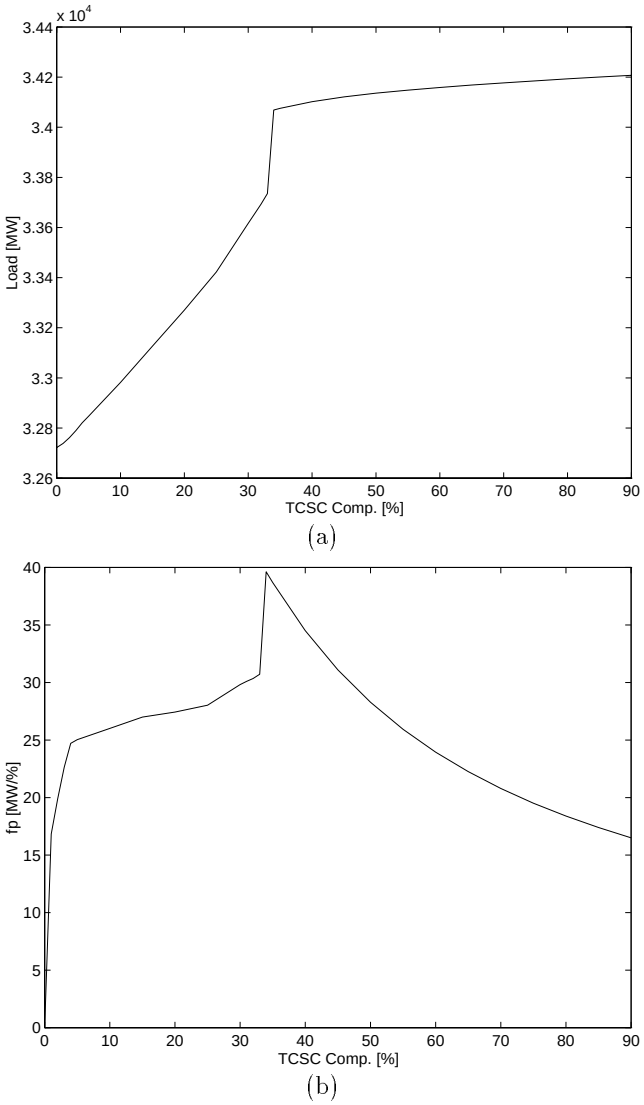

Fig. 12. Effect of changing TCSC compensation levels for critical line 409-436 in (a) loading margin and (b) performance measure fp.

V. Acknowledgments

The authors would like to thank Prof. John Reeve from the University of Waterloo for his observations and suggestions. The research presented here has been conducted with financial support from NSERC.

References

[1] L. H. Fink, editor, *Proc. Bulk Power System Voltage Phenomena III—Voltage Stability and Security*, ECC Inc., Fairfax, VA, August 1994.

[2] Y. Mansour, editor, "Suggested techniques for voltage stability analysis," technical report 93TH0620-5PWR, IEEE/PES, 1993.

[3] P. Kundur, editor, "Voltage stability assessment, procedures and guides," technical report second draft, IEEE/PES Power Systems Stability Subcommittee, 1997. Available at http://www.power.uwaterloo.ca.

[4] I. Dobson and H. D. Chiang, "Towards a theory of voltage collapse in electric power systems," *Systems & Control Letters*, vol. 13, 1989, pp. 253–262.

[5] C. A. Cañizares, F. L. Alvarado, C. L. DeMarco, I. Dobson, and W. F. Long, "Point of collapse methods applied to ac/dc power systems," *IEEE Trans. Power Systems*, vol. 7, no. 2, May 1992, pp. 673–683.

[6] T. Van Cutsem, "A method to compute reactive power margins with respect to voltage collapse," *IEEE Trans. Power Systems*, vol. 6, no. 1, February 1991, pp. 145–156.

[7] J. Lu, C. W. Liu, and J. S. Thorp, "New methods for computing a saddle-node bifurcation point for voltage stability analysis," *IEEE Trans. Power Systems*, vol. 10, no. 2, May 1995, pp. 978–989.

[8] C. J. Parker, I. F. Morrison, and D. Sutanto, "Application of an optimization method for determining the reactive margin from voltage collapse in reactive power planning," *IEEE Trans. Power Systems*, vol. 11, no. 3, August 1996, pp. 1473–1481.

[9] C. A. Cañizares, "Calculating optimal system parameters to maximize the distance to saddle-node bifurcations," accepted for publication in the *IEEE Trans. Circuits and Systems—I*, May 1997.

[10] R. P. Klump and T. J. Overbye, "A transmission-based voltage stability measure for available transfer capability (atc) calculations," *Proc. NAPS*, MIT, November 1996, pp. 351–357.

[11] A. R. Bergen, *Power Systems Analysis*. Prentice-Hall, New Jersey, 1986.

[12] D. Maratukulam, editor, *Proc. FACTS Conference I—The Future in High-voltage Transmission*, TR-100504, EPRI, March 1992.

[13] L. Gyugyi, "Dynamic compensation of ac transmission lines by solid-state synchronous voltage sources," *IEEE Trans. Power Delivery*, vol. 9, no. 2, April 1994, pp. 904–911.

[14] Y. Mansour, W. Xu, F. Alvarado, and C. Rinzin, "SVC placement using critical modes of voltage instability," *IEEE Trans. Power Systems*, vol. 9, no. 2, May 1994, pp. 757–763.

[15] L. A. S. Pilotto, W. W. Ping, A. R. Carvalho, A. Wey, W. F. Long, F. L. Alvarado, C. L. DeMarco, and A. Edris, "Determination of needed facts controllers that increase asset utilization of power systems," *IEEE Tans. Power Delivery*, vol. 12, no. 1, January 1997, pp. 364–371.

[16] Z. T. Faur and C. A. Cañizares, "Effects of FACTS devices on system loadability," *Proc. North American Power Symposium*, Bozeman, Montana, October 1995, pp. 520–524.

[17] S. Greene, I. Dobson, and F.L. Alvarado, "Sensitivity of the loading margin to voltage collapse with respect to arbitrary parameters," *IEEE Trans. Power Systems*, vol. 12, no. 1, February 1997, pp. 262–272.

[18] C. A. Cañizares, "Conditions for saddle-node bifurcations in ac/dc power systems," *Int. J. of Electric Power & Energy Systems*, vol. 17, no. 1, February 1995, pp. 61–68.

[19] C. A. Cañizares and F. L. Alvarado, "Point of collapse and continuation methods for large ac/dc systems," *IEEE Trans. Power Systems*, vol. 8, no. 1, February 1993, pp. 1–8.

[20] I. Dobson, "The irrelevance of load dynamics for the loading margin to voltage collapse and its sensitivities," pp. 509–518 in [1].

[21] I. Dobson and L. Lu, "Voltage collapse precipitated by the immediate change in stability when generator reactive power limits are encountered," *IEEE Trans. Circuits and Systems—I*, vol. 39, no. 9, September 1992, pp. 762–766.

[22] P. A. Löf, G. Andersson, and D.J. Hill, "Voltage dependent reactive power limits for voltage stability studies," *IEEE Trans. Power Systems*, vol. 10, no. 1, February 1995, pp. 220–228.

[23] L. Gyugyi, "Power electronics in electric utilities: Static var compensators," *Proceedings of the IEEE*, vol. 76, no. 4, April 1988, pp. 483–494.

[24] N. Christl, R. Heiden, R. Johnson, P. Krause, and A. Montoya, "Power system studies and modeling for the Kayenta 230 KV substation advanced series compensation," *AC and DC Power Transmission IEEE Conference Publication 5: International Conference on AC and DC Power Transmission*, September 1991, pp. 33–37.

[25] Z. T. Faur. Effects of FATCS devices on static voltage collapse phenomena. Master's thesis, University of Waterloo, 1996. Available at http://www.power.uwaterloo.ca.

[26] I.A. Erinmez,editor, "Static Var Compensators," technical report of task force 2, CIGRE, 1986.

[27] Committee on Static Compensation, *Static Compensators for Reactive Power Control*. Canadian Electrical Association, 1984.

[28] S. G. Jalali, R. A. Hedin, M. Pereira, and K. Sadek, "A stability model for the advanced series compensator (ASC)," *IEEE Trans. Power Delivery*, vol. 11, no. 2, April 1996, pp. 1128–1137.

Claudio A. Cañizares (S'87, M'92) was born in Mexico, D.F. in 1960. He received the Electrical Engineer diploma (1984) from the Escuela Politécnica Nacional (EPN), Quito-Ecuador, where he held different positions from 1983 to 1993. His MS (1988) and PhD (1991) degrees in Electrical Engineering are from the University of Wisconsin–Madison, where he attended as an EPN, OAS and Fulbright Scholar. Dr. Cañizares is currently an Assistant Professor at the University of Waterloo and his research activities are mostly concentrated in computational, modeling, and stability issues in ac/dc/FACTS systems. He is a Professional Engineer in the province of Ontario, Canada, and an active member of IEEE, CIGRE and Sigma Xi.

Zeno T. Faur was born in Romania, Cluj in 1963. In 1988 he graduated from the Technical University of Cluj with a degree in Electrical Engineering. From 1988 to 1993 he worked in the power industry in Romania. In 1991 he attended a specialized training program at EEF, Switzerland for SCADA systems. He graduated with a M.A.Sc. degree from University of Waterloo in January, 1996. His research interests are mainly in studying the effect of FACTS controllers in bifurcations of power systems. Mr. Faur is currently a Project Manager at SAF Drive Systems Ltd. in Kitchener, ON.